<연구논문>

Enhancement of Surface Diffusivity for Waviness Evolution on Heteroepitaxial Thin Films

Yun Young Kim[*]

Department of Mechanical Engineering, Northwestern University, Evanston, Illinois 60208, USA

Abstract

The present study deals with a numerical analysis on the island growth of heteroepitaxial thin-films through local surface diffusivity enhancement. A non-linear governing equation for the surface waviness evolution in lattice-mismatched material systems is developed for the case of spatially-varying surface diffusivity. Results show that a flat film that is stable under constant diffusivity conditions evolves to form nanostructures upon externally-induced spatial diffusivity modulation. The periodicity of waviness can be controlled by changing the modulation parameters, which allows for generation of pattern arrays. The present study therefore points towards a post-deposition treatment technique that achieves controllability and order in the structure formation process for applications in nanoelectronics and thin-film devices.

Keywords: heteroepitaxy, thin film, surface diffusivity, instability

1. INTRODUCTION

Island formation on heteroepitaxial thin-films has been a topic of great interest in recent decades because of its potential for applications in nano-electronics. In a lattice-mismatched material system, such as a silicon-germanium (SiGe) thin-film, the lattice constants of silicon (Si) and germanium (Ge) are 5.43 Å and 5.64 Å at 300 K, respectively, and the mismatch induces elastic strain in the film when a Ge layer is deposited on a Si wafer. The film initially grows layer-by-layer for the first few mono-layers (ML), but above a critical thickness, which is typically 3 MLs for a 100 % Ge film, islands coalesce due to the stronger interactions between adatoms than the bonding between the adatom and the surface. This islanding behavior is known as the Stranski-Krastanov growth[1], and evolution of the structure is attributable to the energy minimization in the material system to relax the elastic strain energy in the film at the expense of increase surface energy.

The nanoscale island structures have attractive optoelectronic properties such as discrete atom-like energy levels, thermal stability, delta-function-like density of states, and highly reproducible transport behavior[2]. Especially with the increasing interest in renewable and sustainable energy, many innovative ideas have been proposed to incorporate such nanostructures into solar-energy conversion devices. One example would be the quantum-dot (QD) solar-cell. When QDs are regularly positioned in the cell design, intermediate-band (IB) or miniband structures are formed to reduce thermalization and transmission loss, and as a result the solar-cell efficiency is enhanced[3]. Investigations show that the maximum power conversion efficiency can be theoretically as high as 45% for a QD solar-cell that has 10~20 layers of indium-arsenide (InAs) QDs encapsulated by an aluminum-gallium-arsenide (AlGaAs) high potential barrier fence under AM1.5 spectral radiation.[4] Although experimental studies[5-8] at the current stage show lower efficiencies, mostly ranging from 7 to 12%, another theoretical study predicts that it can be as high as 25 ~ 50% depending on the precise control of QD dimension and gallium content

*Corresponding Author : Yun Young Kim
Department of Mechanical Engineering, Northwestern University
E-mail : y.kim@u.northwestern.edu

in $In_xGa_{1-x}N/GaN$ QD IB solar-cells.[9]

Thus, achieving dimensional uniformity in the island formation is important for device fabrication since the size and distribution affect performance. In addition, reproducibility is also a requirement for quality-control issues in manufacturing. However, the spontaneous structure formation process observed in lattice-mismatched material systems is mainly governed by stress-driven mass diffusion, which is inherently a statistical process that results in an element of randomness, and this is detrimental to device realization. While many approaches to regularize the pattern formation depend on strain-engineering methods that make use of photolithographically-predefined substrates,[10-12] these require repetitive fabrication process steps, and may limit the choice of substrates. Therefore, instead of using those energetically-favored growth methods, a different route is needed to kinetically form the islands through a local diffusivity modulation.

Here, a numerical study is presented to demonstrate that a periodic temperature distribution, which could be obtained by localized heating, enhances the surface diffusivity of an initially flat and strained film, perturbing the morphology to self-assembled regular nanostructure arrays. The governing equation that describes the structure growth under the diffusivity modulation is formulated, and conditions for the numerical implementation are presented. Results obtained from the proposed approach are discussed, and effects of various modulation conditions are also assessed.

2. EVOLUTION EQUATION

The mathematical domain of analysis is defined such that the film with the slightly larger lattice parameter is located in the region $0 < z < h(x,y,t)$ on a substrate as shown in Fig. 1. Studies[13-15] have
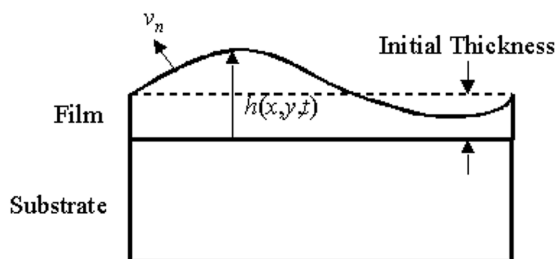

Fig. 1. Problem description. The morphology of an initially flat and strained film is evolving with a normal velocity of v_n. The film and substrate are elastic materials in a continuum space.

shown that the initially flat film is strained due to the lattice-mismatch, and it is morphologically unstable. Therefore, the surface undulates to find a steady-state shape as the material system seeks to lower its energy. The process is known to occur through stress-driven surface diffusion of atoms. Assuming that the film is dislocation-free, the mass flux can be written as follows:

$$\vec{j} = -\frac{D_s c_s}{k_b \theta} \nabla_s \chi \qquad (1)$$

where D_s is the surface diffusivity, c_s is the concentration of diffusing species, k_b is the Boltzmann constant, θ is the surface temperature, and χ is the surface chemical potential. Previous studies[13-15] considered D_s and θ as spatially constant, supposing that the whole film is uniformly annealed in an oven or furnace. In the present approach, however, a situation is considered such that a source of local perturbation is provided to impose spatially-periodic surface temperature boundary conditions. The surface temperature is then a function of spatial variables, x and y. Accordingly, D_s in the Arrhenius form is modified as:

$$D_s(x,y) = D_0 \exp\left[-\frac{E_d}{k_b \theta(x,y)}\right] \qquad (2)$$

where D_0 is the pre-exponential factor and E_d is the activation barrier for surface diffusion. Then Eq. (1) is modified as:

$$\vec{j} = -\frac{D_s(x,y)c_s}{k_b \theta(x,y)} \nabla_s \chi \qquad (3)$$

Regarding the chemical potential, χ, it is well known that the evolution of the film morphology is a result of competition between the surface free energy and elastic strain energy.[13] Research[16] showed that the introduction of a wetting term in χ reduces numerical difficulties by considering the discrete change of surface energy across the film-substrate interface as a smooth and continuous function within a transition boundary-layer. Therefore, the surface chemical potential is taken as:

$$\chi = [U - \gamma_F \kappa + \omega]\Omega \qquad (4)$$

where Ω is the atomic volume. Here, specific forms of mathematical representation for strain energy (U), surface energy ($\gamma_F\kappa$), and wetting energy (ω) follow what are proposed in Ref. 17:

$$U = \frac{1}{2}\sigma_{ij}^F E_{ij}^F \quad \text{on } z = h(x,y,t) \tag{5}$$

$$\kappa = -\frac{(1+h_y^2)h_{xx} - 2h_x h_y h_{xy} + (1+h_x^2)h_{yy}}{(1+h_x^2+h_y^2)^{3/2}} \tag{6}$$

$$\omega(h) = \frac{-1}{\sqrt{1+|\nabla h|^2}}\frac{\Delta\gamma}{\pi}\frac{\delta}{\delta^2+h^2} \tag{7}$$

where σ_{ij}^F and E_{ij}^F are the stress and linear elasticity strain tensors in the film, $\Delta\gamma$ is the difference between the film and substrate surface energies, and δ is the transition boundary-layer thickness.

Assuming that there is no incoming flux of atoms onto the surface, and the film deposition has been completed, the normal velocity of surface height growth due to diffusion driven morphology change is expressed as:

$$v_n = -\Omega\nabla_s \cdot \vec{j} \tag{8}$$

Incorporating Eq. (3) into Eq. (8) leads to the growth equation:

$$\frac{\partial h}{\partial t} = \frac{\Omega^2 c_s}{k_b}\sqrt{1+|\nabla h|^2}\left\{\nabla_s\left(\frac{D_s}{\theta}\right)\cdot\nabla_s\chi + \left(\frac{D_s}{\theta}\right)\nabla_s^2\chi\right\} \tag{9}$$

Suppose that a spatially-periodic surface temperature variation is provided so that D_s/q is approximated as:

$$\frac{D_s}{\theta} \approx \overline{D_0}(1+\varepsilon_D\cos(2\pi x/\lambda_D)) = \overline{D_0}\widehat{D}_s \tag{10}$$

where $\overline{D_0}$ is the mean of D_s/q, ε_D is the amplitude of the diffusivity variation, and l_D is the wavelength of the modulation profile. One can easily obtain such conditions using laser-beam interference patterns or a spatial-light modulator, resulting in a sinusoidal surface temperature profile that locally enhances the surface diffusivity where higher-intensity fringes are illuminated. Normalization of Eq. (9) results in a dimensionless governing equation as:

$$\frac{\partial H}{\partial T} = \nabla_s\widehat{D}_s\cdot\nabla_s\left[\tilde{\varepsilon}_1(H) - \nabla^2 H - \frac{r}{H}\right] + \widehat{D}_s\nabla_s^2\left[\tilde{\varepsilon}_1(H) - \nabla^2 H - \frac{r}{H}\right] \tag{11}$$

Expressions for $\tilde{\varepsilon}_1(H)$ and r are presented in detail in Refs. 15 and 17. Eq. (11) shows that the diffusivity modulation affects the velocity of surface

waviness growth. If D_s and q are spatially constant, then the first term on the right hand side of Eq. (11) disappears and the growth is only influenced by the chemical potential term, .

3. NUMERICAL IMPLEMENTATION

For the numerical solution of Eq. (11), the central finite difference formula with fourth-order accuracy and the backward differentiation formulas (BDFs, also known as the Gear's method) were employed for discretization in space and evolution in time, respectively. The total number of spatial nodal points are 72×72 in space and the normalized time step is $\Delta T = 0.01$. A periodic boundary condition was applied. Material parameters were taken for an example of a $Si_{0.5}Ge_{0.5}$ film on a Si substrate, and the weighted average of 100% Si and Ge properties were used for the film. The shear moduli of the film and substrate are $\mu_F = 45.7$ GPa and $\mu_S = 50.9$ GPa, respectively. Poisson's ratios of the film and substrate are $v_F = 0.276$ and $v_S = 0.278$, respectively. In this case, the elastic energy density leads to $U_0 = 2\varepsilon_0^2\mu_F(1+v_F)/(1-v_F) = 64.4$ MPa, where ε_0 is the biaxial elastic strain, $\varepsilon_0 = (a_S-a_F)/a_F$. The lattice parameter of $Si_{0.5}Ge_{0.5}$ film is 5.55 Å. The surface energies of the film and substrate are taken to be $\gamma_F = 2.220$ J/m^2 and $\gamma_S = 2.513$ J/m^2, respectively. The transition boundary layer thickness, δ, is 0.012 nm, and the characteristic film thickness is $H_0 = 4$ nm. A steady-state solution was deemed to be achieved when the average growth rate at a certain time step was less than 1 % of the initial growth rate:

$$\left.\frac{d\overline{H}}{dT}\right|_{normalized} = \frac{\sum_{i=1}^{n}\left|\frac{dH(X_i,T)}{dT}\right|}{\sum_{i=1}^{n}\left|\frac{dH(X_i,T_0)}{dT}\right|} < 0.01 \tag{12}$$
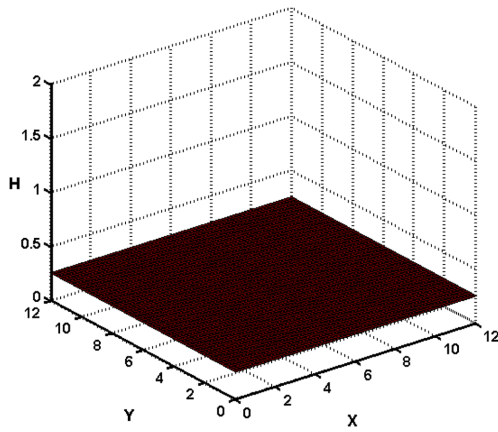
where n is the total number of nodal points.

4. RESULTS AND DISCUSSION

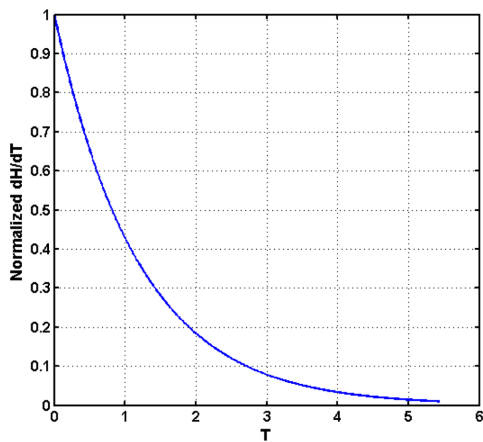### 4.1. Uniform surface diffusivity under a stable regime

An initial perturbation of the height is chosen in the form:

$$H = H_0 + \varepsilon_h\cos[(\sqrt{2}\pi/\Lambda_h)(X-Y)] \cos[(\sqrt{2}\pi/\Lambda_h)(X+Y-\Lambda_h)] \tag{14}$$
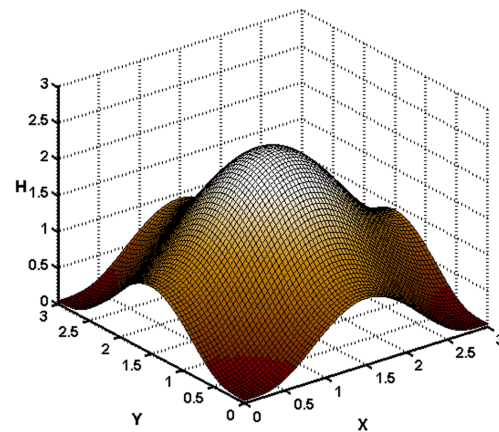
(a)

(b)

Fig. 2. The growth behavior of a film under stable regime. (a) The morphology remains flat and did not evolve. (b) The normalized average growth rate decreases below 1%.
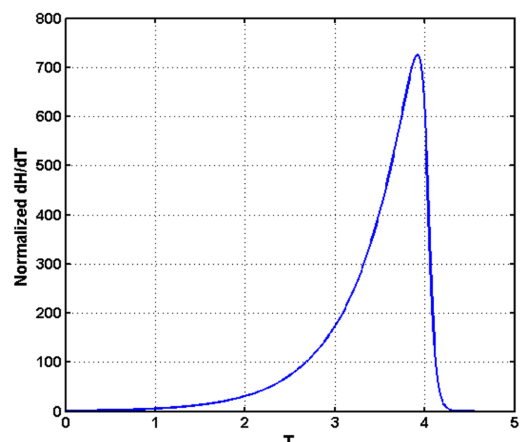

(a)

(b)

Fig. 3. Surface waviness evolution under unstable regime. (a) A pattern emerges when the film is thick enough under constant diffusivity conditions. (b) Corresponding growth rate changes with respect to time.

where the parameters were chosen such that $H_0 = 0.25$, $\varepsilon_h = 10^{-3}$, and $\Lambda_h = 3.0$ for validation. Based on a stability analysis,[15] it is known that for the parameters under consideration the film is always stable under a critical thickness (H_c) and over a critical wavenumber ($\Lambda_c = 2p\,\Lambda_c$) and as such the perturbations should not grow under these conditions. As shown in Fig. 2(a), the numerical simulation indeed shows that the surface does not grow with respect time. The normalized average growth rate in Fig. 2(b) depicts that the amplitude drops below 1% and the morphology change is negligible afterward. In a similar way, the film is always planar for any Λ_h at a critical thickness ($H_c = 0.19$ in our case) as well as any H over a critical wavenumber ($\Lambda_c > 2.29$ or $\Lambda_h < 2.7$).

4.2. Uniform surface diffusivity under an unstable regime

Next, the film thickness was increased to $H_0 = 1.0$

while other parameters were kept the same ($\varepsilon_h = 10^{-3}$ and $\Lambda_h = 3.0$) so that the initial perturbation falls into the unstable regime. Figure 3(a) reveals that a pattern emerges even with constant diffusivity, just as QDs form on the surface of a SiGe film over the critical thickness. The variation of normalized average growth rate with respect to time is presented in Fig. 3(b). The growth is accelerated until $T = 3.92$ but slows down until it reaches a steady-state at $T = 4.55$.

4.3. Pattern formation on a stable film through surface diffusivity modulation

From now on, a case is considered in which the system is expected to be stable under constant diffusivity. Initial perturbation parameters are still $H_0 = 0.25$, $\varepsilon_h = 10^{-3}$, and $\Lambda_h = 3.0$. However, the surface diffusivity is intentionally modulated in various ways. Consider a spatially-varying surface

diffusivity as follows:

$$\widehat{D}_s = 1.0 - 0.1\cos\left(\frac{2\pi X}{12}\right)\left[1 + \sin\left(\frac{2\pi(Y-\Lambda_D)}{12}\right)\right] \quad (16)$$

A result for the diffusivity modulation of $\Lambda_D = 3.0$ is presented in Fig. 4(a). The modulation condition is graphically presented in the inset. Unlike the case of constant diffusivity in Fig. 2(a), patterns self-assemble on the initially flat film. When Λ_D was changed from 3.0 to 1.5, the periodicity of steady-state structure again followed that of the modulation in Fig. 4(b). In additional examples, spot-modulation conditions were provided through a combination of sinusoidal functions in two dimensions for the local diffusivity enhancement, and again the modulation guided the growth of structures, leading to ordered arrays on the film as illustrated in Figs. 4(c) and 4(d). Since no incoming flux of atoms was assumed in the problem description, mass conservation is maintained within the domain of analysis, and thus the amplitude of patterns decreases as the number of islands increases in the area.

Regarding the stability of the evolved steady-state patterns, a question may arise whether the obtained island pattern goes back to a flat film once the externally induced diffusivity modulation stops.
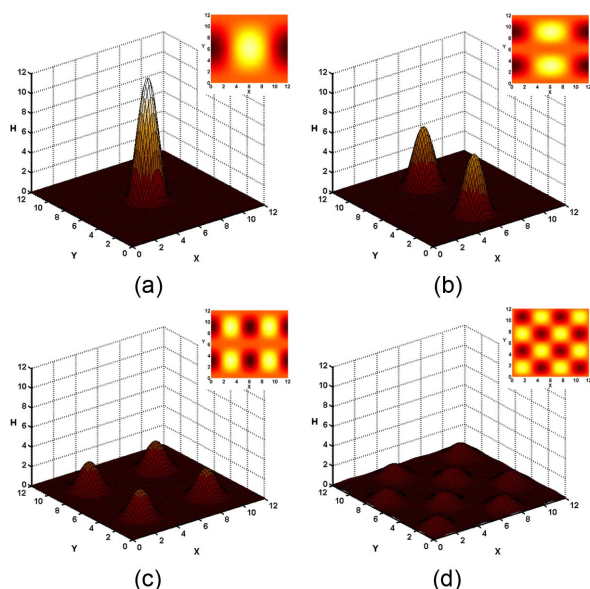
However, an examination of the chemical potential gradient at the steady-state reveals that it has reached to a near-zero value and there is no further driving force for the surface diffusion. As an illustration, Fig. 5 presents the change of normalized root-mean-square (RMS) of the chemical potential gradient with respect to time. During the surface waviness evolution the chemical potential gradient eventually drops to a very small value. Since $\tilde{N}\chi = 0$, the right-hand side of Eq. (11) tends to zero and there is no change of surface height with respect to time. To confirm that the morphology is not evolving any further, the steady-state solution was taken as an initial perturbation and fed into the governing equation for the case of *constant* diffusivity. As expected, the calculation did not proceed any more. From an experimental point of view, this foresees that a post-deposition thermal treatment can produce nanostructures on a flat SiGe surface by locally enhancing the surface diffusivity. Also, as opposed to the strain-engineering method,[10-12] this approach will simplify the pattern formation process by eliminating the need for pre-defined substrates that require repetitive fabrication steps.

5. SUMMARY

A concept is numerically validated such that an island formation is initiated and aligned via local surface diffusivity enhancement in this study. Taking

Fig. 4. Growth of ordered quantum-dot arrays. The specific diffusivity modulation conditions are (a) $\widehat{D}_s$ = 1.0 − 0.1cos(2πX/12)[1 + sin[2π(Y−3)/12]] (b) $\widehat{D}_s$ = 1.0 − 0.1cos(2πX/12)[1 + sin[2π(Y−1.5)/6]] (c) $\widehat{D}_s$ = 1.0 − 0.1cos(2πX/6)[1 + sin[2π(Y−1.5)/6]] (d) $\widehat{D}_s$ = 1.0 − 0.1sin(2πX/6)sin(2πY/6). Insets show graphical representation of local diffusivity modulation.
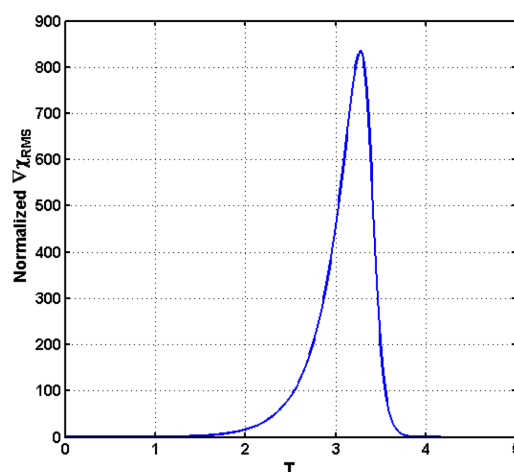

Fig. 5. The normalized RMS of the chemical potential gradient with respect to time. Note that this becomes a near-zero value, confirming that there is no further driving force for the growth and accordingly the morphology will not return to the flat surface after the diffusivity modulation stops.

the temperature-induced spatially-varying diffusivity into account, a governing equation was formulated and simulations on the morphology evolution were performed. Results show that with the local diffusivity modulation structures are formed even on a flat film under a stable regime which otherwise would have not grown under constant diffusivity conditions. Also, by taking advantage of the spatial selectivity in the patterning process, ordered patterns can be generated with the adjustment of diffusivity modulation conditions. The present study suggests a possible way to regularize island structures in lattice-mismatched material systems by a post-deposition laser-treatment, leading to a simplified fabrication technique for applications in a lattice-mismatched materials system.

References

1. I. N. Stranski and L. Krastanov : Sitzungsber. Akad. Wiss. Wien, Math.-Naturwiss. Kl., Abt. 2B, **146**(1938) 797.

2. S. Oda and D. Ferry : Silicon nanoelectronics, CRC Press, Boca Raton (2006).

3. T. Markvart and L. Castaner : Solar Cells: Materials, Manufacture and Operation, Elsevier, Amsterdam (2005).

4. G. Wei and S. R. Forrest : Nano Letters 7 (2007) 218.

5. K. A. Sablon, J. W. Little, K. A. Olver, Zh. M. Wang, V. G. Dorogan, Yu. I. Mazur, G. J. Salamo, and F. J. Towner : J. Appl. Phys. 108 (2010) 074305.

6. T. Sugaya, S. Furue, H. Komaki, T. Amano, M. Mori, K. Komori, S. Niki, O. Numakami, and Y. Okano : Appl. Phys. Lett. 97 (2010), 183104.

7. Y. Okada, T. Morioka, K. Yoshida, R. Oshima, Y. Shoji, T. Inoue, and T. Kita : J. Appl. Phys. 109 (2011) 024301.

8. T. Sugaya, Y. Kamikawa, S. Furue, T. Amano, M. Mori, and S. Niki : Solar Energy Mater. Solar Cells 95 (2011) 163.

9. Q. Deng, X. Wang, C. Yang, H. Xiao, C. Wang, H. Yin, Q. Hou, J. Li, Z. Wang, and X. Hou: Physica B 406 (2011) 73.

10. S. J. Koh : Nanoscale Res. Lett. 2 (2007), 519.

11. C. Dais, H. H. Solak, E. Müller, and D. Grützmacher : Appl. Phys. Lett. 92 (2008) 143102.

12. R. Nötzel, N. Sritirawisarn, E. Selçuk, and S. Anantathanasarn: IEEE J. Sel. Top. Quant. Electron. 14 (2008) 1140.

13. H. Gao and W. D. Nix : Annu. Rev. Mater. Sci. 29 (1999) 173.

14. L. B. Freund : Int. J. Solids Structures 32(1995), 911

15. W. T. Tekalign and B. J. Spencer : J. Appl. Phys. 96 (2004) 5505.

16. B. J. Spencer : Phys. Rev. B 59(1999), 2011

17. W. T. Tekalign and B. J. Spencer : J. Appl. Phys. 102 (2007) 073503.

18. Y.Y. Kim, Q. Huang, and S. Krishnaswamy: Appl. Phys. Lett. 96 (2010) 123116.

19. C. Zhang and R. Kalyanaraman: Appl. Phys. Lett. 83 (2003) 4827.